Experimental Hematology

ARTICLE
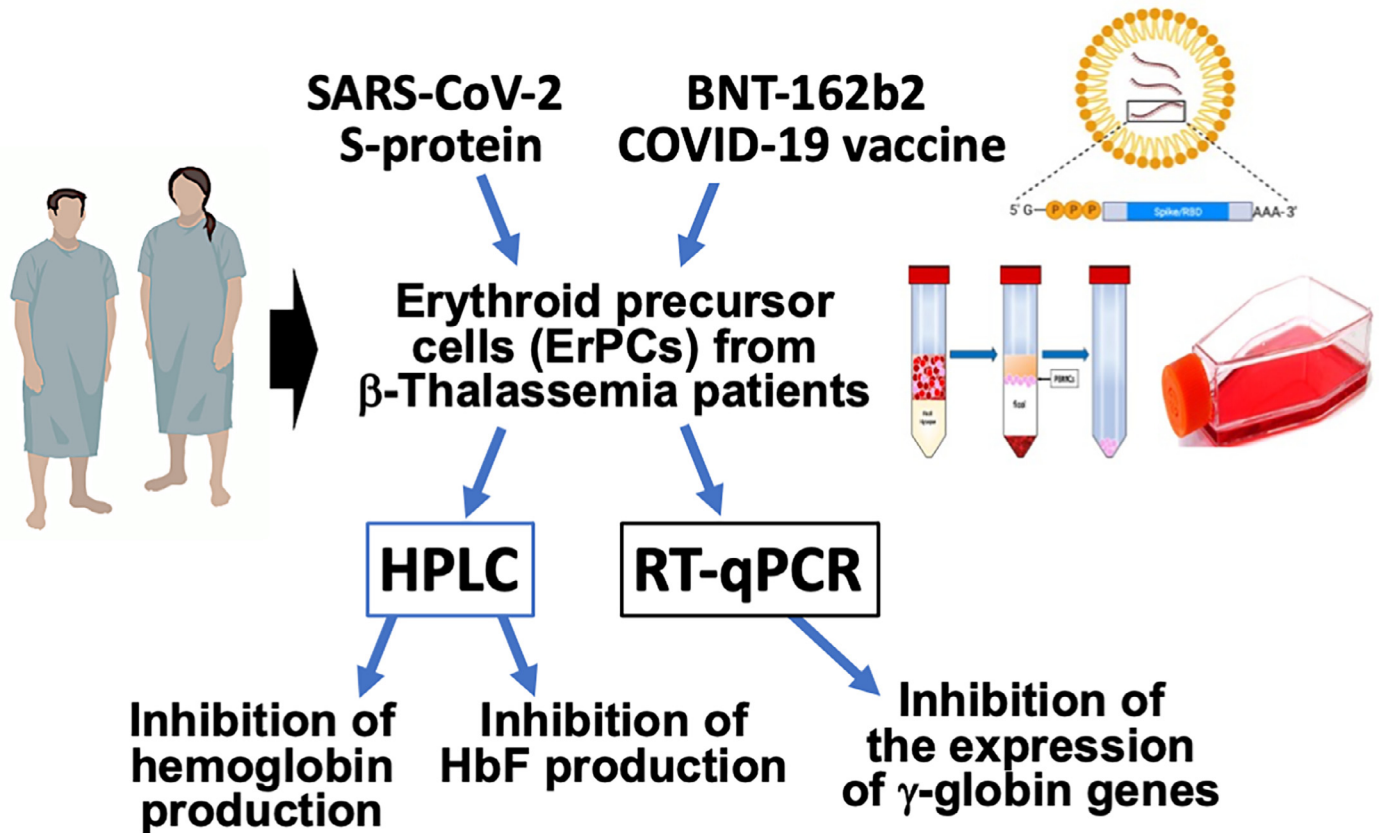
ISEH
INTERNATIONAL SOCIETY FOR
EXPERIMENTAL HEMATOLOGY

Inhibitory effects of SARS-CoV-2 spike protein and BNT162b2 vaccine on erythropoietin-induced globin gene expression in erythroid precursor cells from patients with β-thalassemia

ARTICLE

Inhibitory effects of SARS-CoV-2 spike protein and BNT162b2 vaccine on erythropoietin-induced globin gene expression in erythroid precursor cells from patients with β-thalassemia

Lucia Carmela Cosenza[a], Giovanni Marzaro[b], Matteo Zurlo[a], Jessica Gasparello[a], Cristina Zuccato[a,c], Alessia Finotti[a,c], and Roberto Gambari[a,c]*

[a]*Department of Life Sciences and Biotechnology, Section of Biochemistry and Molecular Biology, University of Ferrara, Ferrara, Italy;* [b]*Department of Pharmaceutical and Pharmacological Sciences, University of Padova, Padova, Italy;* [c]*Center "Chiara Gemmo and Elio Zago" for the Research on Thalassemia, Department of Life Sciences and Biotechnology, University of Ferrara, Ferrara, Italy*

During the recent coronavirus disease 2019 (COVID-19) pandemic several patients with β-thalassemia have been infected by severe acute respiratory syndrome coronavirus (SARS-CoV-2), and most patients were vaccinated against SARS-CoV-2. Recent studies demonstrate an impact of SARS-CoV-2 infection on the hematopoietic system. The main objective of this study was to verify the effects of exposure of erythroid precursor cells (ErPCs) from patients with β-thalassemia to SARS-CoV-2 spike protein (S-protein) and the BNT162b2 vaccine. Erythropoietin (EPO)-cultured ErPCs have been either untreated or treated with S-protein or BNT162b2 vaccine. The employed ErPCs were from a β-thalassemia cellular Biobank developed before the COVID-19 pandemic. The genotypes were β^+-IVSI-110/β^+-IVSI-110 (one patient), $\beta^0$39/β^+-IVSI-110 (3 patients), and $\beta^0$39/ $\beta^0$39 (2 patients). After treatment with S-protein or BNT162b2 for 5 days, lysates were analyzed by high performance liquid chromatography (HPLC), for hemoglobin production, and isolated RNA was assayed by RT-qPCR, for detection of globin gene expression. The main conclusions of the results obtained are that SARS-CoV-2 S-protein and BNT162b2 vaccine (a) inhibit fetal hemoglobin (HbF) production by β-thalassemic ErPCs and (b) inhibit γ-globin mRNA accumulation. In addition, we have performed in silico studies suggesting a high affinity of S-protein to HbF. Remarkably, the binding interaction energy of fetal hemoglobin to S-protein was comparable with that of angiotensin-converting enzyme 2 (ACE2). Our results are consistent with the hypothesis of a relevant impact of SARS-CoV-2 infection and COVID-19 vaccination on the hematopoietic system. © 2023 ISEH – Society for Hematology and Stem Cells. Published by Elsevier Inc. This is an open access article under the CC BY-NC-ND license (http://creativecommons.org/licenses/by-nc-nd/4.0/)

HIGHLIGHTS

- The severe acute respiratory syndrome coronavirus (SARS-CoV-2) is responsible for the ongoing coronavirus disease 2019 pandemic.

- The SARS-CoV-2 S-protein is responsible for the side effects of RNA-based vaccines.

- The S-protein inhibits fetal hemoglobin (HbF) in β-thalassemia erythroid precursors.

- S-protein and BNT162b2 vaccine inhibit γ-globin mRNA accumulation.

- In silico studies demonstrate that the S-protein exhibits high affinity to HbF.

Since its spread at the beginning of 2020, the coronavirus disease 2019 (COVID-19) pandemic represents one of the major health problems, causing radical changes in the behavior of the society and forcing research efforts to develop novel therapeutic options [1−3]. Several studies have been focused on possible effects of severe acute respiratory syndrome coronavirus (SARS-CoV-2) infection on hematologic parameters [4−7]. Following the approval of the anti−SARS-CoV-2 vaccines by the Regulatory Agencies (European Medicine Agency [EMA] in Europe and Food and Drug Administration (FDA) in United States) COVID-19 vaccines have been extensively tested and distributed worldwide [8−10]. Because the COVID-19 pandemic is not over, we expect that the vaccination campaign will continue [11]. Accordingly, it is time for evaluation of the short- and long-term effects of the vaccines to have more information about possible effects (including toxicity) on human tissue systems [11].

Concerning this issue, several studies sustain the concept that the SARS-CoV-2 spike protein (S-protein) is a major factor accounting for side effects of the COVID-19 mRNA vaccines [11−16], such as the BNT162b2 from Pfizer-BioNTech [17,18] and the mRNA-1273 from Moderna [19]. This was recently discussed by Trougakos et al. [12], who suggested that COVID-19 mRNA vaccine-induced S-protein was responsible of the majority of adverse effects following vaccination [13].

In this respect, there is a general agreement that the S-protein affects cellular metabolism and gene expression in several tissue systems [20−27]. For instance, several articles demonstrated a "toxic" effect of the S-protein on different cellular systems, such as cardiomyocytes [20], cardiac pericytes [21], endothelial cells [22,23], and hematopoietic cells [24,25]. In this context, Ropa et al. [24] performed ex vivo experiments demonstrating that hematopoietic stem cells (HSCs) and hematopoietic progenitor cells (HPCs) display low-efficient expansion and less-functional colony-forming capacity when exposed ex vivo to the SARS-CoV-2 S-protein. Because these effects occur when HSCs and HPCs are exposed to the recombinant S-protein alone, being the infection by SARS-CoV-2 virus not necessary, it was suggested that SARS-CoV-2 may impact HSCs/HPCs via S-protein interactions with the cells, even in the absence of a true viral infection [24]. In addition, Kucia et al. [25] reported that the S-protein damages hematopoietic stem/progenitor cells activating the mechanism of pyroptosis.

The impact of S-protein on cellular functions is of key interest because the 2 mRNA vaccines BNT162b2 from Pfizer-BioNTech and mRNA-1273 from Moderna, generate high levels of spike [11,13,18,26,27]. Therefore, searching for circulating spike in plasma of patient with COVID-19 might help in understanding unexpected adverse effects following COVID-19 mRNA vaccination. For instance, Yonker et al. [14] were able to identify circulating S-protein in post-COVID-19 mRNA vaccine myocarditis. Persistent circulating SARS-CoV-2 spike was recently proposed to be causative of the COVID-19-associated syndrome termed postacute sequelae of COVID-19 (PASC) [28−31].

Considering that the anti-SARS vaccination campaigns are expected to be ongoing for the next coming years [9], extensive analysis of the effects of spike in ex vivo cellular systems is required for understanding possible impacts on vaccination [11−13].

In some cases, the effects of SARS-CoV-2 infection and/or vaccination should be carefully considered, especially with respect to the hematopoietic system. In this respect, Estep et al. [32] found that SARS-CoV-2 infection and COVID-19 vaccination dramatically impair the functionalities and survivability of hematopoietic stem progenitor cells (HSPCs) in the umbilical cord blood.

The objective of this study was to determine the impact (if any) of SARS-CoV-2 S-protein and an RNA vaccine (the BNT162b2) on erythroid precursor cells (ErPCs) [33] isolated from patients with β-thalassemia. In particular, we focused on possible alterations of gene expression studied by RT-qPCR and hemoglobin production studied by high performance liquid chromatography (HPLC) [34,35].

METHODS

In Vitro Culture of CD34+-ErPCs from Patients with β-Thalassemia

We have employed samples from the THALAMOSS (THALAssaemia MOdular Stratification System for personalized therapy of beta-

Table 1 Genotype of recruited patients and treatment of CD34+-ErPCs with the SARS-CoV-2 S-protein

Patient #	Genotype	Treatment of ErPCs with SARS-CoV-2 spike	Treatment of ErPCs with BNT162b2 vaccine
#1	β^+IVS1-110/β^+-IVS1-110	X	X
#2	β^+-IVS1-110/β^0-39	X	
#3	β^+-IVS1-110/β^0-39	X	
#4	β^0-39/β^0-39	X	
#5	β^+-IVS1-110/β^0-39	X	
#6	β^0-39/β^0-39		X

Abbreviations: ErPC=Erythroid precursor cells; SARS-CoV-2 S-protein=severe acute respiratory syndrome coronavirus 2 spike protein.

thalassemia) cellular Biobank, developed, validated, and described by Cosenza et al. [36]. Biobanked CD34+-ErPCs were selected from 6 patients exhibiting different genotypes (Table 1). In our experiments, the purity of these CD34+-ErPCs is higher than 95% [36].

Patients have been recruited at the Thalassemia Centre of Azienda Ospedaliera-Universitaria S. Anna (Ferrara, Italy). Informed written consent from all participants was obtained before recruiting them into the study. Biobanked CD34+-ErPCs were thawed in 5 mL of IMDM (Life Technologies) 10 × medium, 5% fetal bovine serum (FBS), and incubated at 37°C with controlled humidity with 5% CO_2 in expansion medium, according to the protocol described by Cosenza et al. [36]. ErPCs differentiation was assessed by benzidine staining [35].

Treatment with S-Protein and the BNT162b2 Vaccine

After recovering from the thawing, the CD34+-ErPCs have been treated with SARS-CoV-2 S-protein (139 kDa; stock concentration = 7.2 μM in 9% urea, 0.32% Tris−HCl pH 7.2, 50% glycerol) to achieve the final concentrations of 1−25 nM accordingly with elsewhere reported studies [37−39]. To maximize S-protein interaction with the receptor and the S-protein cellular uptake, the cells were incubated with the S-protein for a first period of 30 min at 4°C, then an incubation for 30 min at 37°C was performed. Internalization of the SARS-CoV-2 S-protein by ErPCs is expected, because the presence of cell surface angiotensin-converting enzyme-2 (ACE2) has been reported in erythroid progenitors [7,24,40,41]. In addition, it has been reported that, apart ACE2, other proteins can facilitate spike binding and entry, such as DPP4, TMPRSS2, Kim-1, NRP-1, CD147, furin, CD209L, and CD26 [42−45]. In any case, the ErPC populations here studied express ACE2, as depicted in Supplementary Figure E1. Importantly, we underline that the level of expression of ACE2 in ErPC approaches that found in the bronchial epithelial Calu-3 cells (Supplementary Figure E1), that can be efficiently infected by SARS-CoV-2, as recently reported by our research group [46,47]. After the second incubation with S-protein, LHC-8 medium supplemented with 5% (final concentration) FBS was added to a final 500 μL volume, and the cultures were further incubated at 37°C and for 24 hours. Then, the S-protein-treated ErPCs were cultured at 37°

C with controlled humidity with 5% CO_2 in the presence of 1 U/mL erythropoietin (EPO), and after 5 days the cells were analyzed.

For treatment with the BNT162b2 vaccine, ErPCs were cultured (10^6 cells/mL, 5 mL) for 24 hours in the presence of EPO. Then ErPCs were either untreated or treated with BNT162b2 (1 μg/mL final concentration) for 5 days. Control experiments were performed to demonstrate the BNT162b2 vaccine-mediated entry of spike-mRNA and the S-protein production by BNT162b2-treated cells. This is shown in Supplementary Figure E2. The presence of relatively high levels of spike-mRNA was clearly detectable after 48 hours treatment (Supplementary Figure E2A). As expected from published studies, the content of spike mRNAs decreases during the culture period. The presence of S-protein was detected by Western blotting assay (Supplementary Figure E2B) and by enzyme-linked immunosorbent assay (ELISA) (Supplementary Figure E2C). Importantly, all the untreated ErPC cultures were negative (S-protein levels undetectable) in the performed ELISA assay; conversely, all the BNT162b2-treated cells displayed release of S-protein.

The BNT162b2 vaccine (COMIRNATY^{TM}, Lot. FP8191) was obtained from the Hospital Pharmacy of University of Padova.

At the end of the cell culture period, cell lysates were prepared according to Zuccato et al. [34] for analysis of the hemoglobin pattern by HPLC, and RNA was isolated for RT-q-PCR and Droplet Digital PCR (ddPCR) studies.

RNA Extraction from ErPCs and RT-qPCR Analysis

The total cellular RNA was extracted from ErPCs by using TRIzolTM LS (Invitrogen) and TRI Reagent (Sigma−Aldrich) following the manufacturers' instructions. The protocol used for extraction of RNA from ErPCs was strictly followed with these steps: (a) dry pellet of 4 −6 × 10^6 ErPCs were diluted in 800 μL of TRI Reagent (added without reverse pipetting to avoid any clumping); and (b) the isolated RNA was washed once with cold 75% ethanol, dried, and dissolved in 10−20 μL nuclease-free water before use.

For gene expression analysis, 500 ng of total RNA was reverse transcribed in complementary DNA (cDNA) by using the TaqMan Reverse Transcription Reagents and random hexamers (Applied Biosystems, Life Technologies).

Quantitative real-time PCR assay, to quantify the gene expression was carried out using 2 different reaction mixtures, the first one containing probe and primers for the gene under study, and the second one containing probes and primers for the housekeeping glyceraldehyde-3-phosphate dehydrogenase (*GAPDH*), *RPL13A*, and β-actin sequences, used as internal controls. The primers and probes used are listed in Table 2.

Each reaction mixture contained 1 × TaKaRa Ex Taq DNA Polymerase (Takara Bio Inc.), 300 nM forward and reverse primers, and 200 nM probes (Integrated DNA Technologies). The assays were carried out using the CFX96 Touch Real-Time PCR System (Bio-Rad). After an initial denaturation at 95°C for 1 min, the reactions were performed for 50 cycles (95°C for 15 sec and 60°C for 60 sec). Data were analyzed by employing the CFX manager software (Bio-Rad). To compare gene expression of each template amplified, the $\Delta\Delta$Ct method was used [34,35].

ddPCR

The evaluation of the ACE2 mRNA in untreated ErPCs was carried out by ddPCR. In these experiments Taq-Man probe, marked with FAM fluorophore, was designed using IDT tools. The predetermined quantity of cDNA was added to ddPCR reaction mix containing 2 × ddPCR Supermix for Probes (no deoxyuridine triphosphate (dUTP)) (Bio-Rad). The ddPCR reaction was mixed with Automated Droplet Generation Oil for Probes (Bio-Rad), and droplets emulsion (water in oil) was automatically generated using Automated Droplet Generator (AutoDG) (Bio-Rad). The emulsion was amplified using GeneAmp PCR System 9700 (Thermo Fisher Scientific) using the following thermal cycler condition at 95°C for 10 min, 94°C for 30 sec and 61°C for 1 min repeated for 40 cycles, then a final phase of inactivation of the enzyme DNA polymerase at 98°C for 10 min was performed. The plate was kept at 4°C for 1 hour before reading to stabilize the analysis. The genereted droplets were read using the QX200 Droplet Reader, and data analysis was performed using QuantaSoft version 1.7.4 (Bio-Rad).

HPLC Analysis of Hemoglobin

To evaluate the effects of treatments on hemoglobin production, HPLC analysis was carried out. The ErPCs were centrifuged at 8,000 rpm for 8 min and washed with phosphate-buffered saline solution (PBS). The pellets were then resuspended in a predefined volume of water for HPLC (Sigma−Aldrich), vortexed at high speed and incubate for 20 min on ice to lyse the cells and obtain the protein extracts. Hemoglobin analysis was performed by loading the protein extracts into a PolyCAT-A cation exchange column and with Beckman Coulter instrument System Gold 126 Solvent Module-166 Detector to obtain a quantification of the hemoglobin present in the sample. The reading was performed at a wavelength of 415 nm, and a commercial solution of purified human HbF (Sigma−Aldrich) extracts was used as standard. The optical density values read in the sample were processed using "32 Karat software."

Western Blotting Analysis

The accumulation of γ-globin, transferrin receptor (CD 71), and SARS-CoV-2 spike S1 proteins in ErPCs cultured in the absence or in the presence of S-protein and BNT162b2 was assessed by Western blotting.

For whole-cell extract preparation, the cells were lysed with RIPA buffer (Thermo Fisher Scientific) following manufacturer's instruction and quantified by bicinchoninic acid (BCA) assay (Pierce^{TM} BCA Protein Assay kit, Thermo Fisher Scientific). For each sample, 20 μg of cell extracts were loaded on 6%−18% hand-casted sodium dodecyl sulfate-polyacrylamide gel electrophores (SDS-PAGE) gradient gel (40% acrylamide/bis-acrylamide solution, Bio-Rad). After separation by electrophoretic run, the proteins were transferred onto 0.2-μm nitrocellulose paper (Protran, Cytiva), and incubated with the primary antibodies listed in Table 3; the constitutive protein β-actin was selected as housekeeping to normalize the quantification of the target proteins.

Membranes were incubated with an appropriate Horseradish peroxidase (HRP)-conjugated secondary antibody (Cell Signalling Technology, cat. no. 7074) and LumiGLO ECL kit (Cell Signaling Technology) was employed following manufacturer's instruction before exposure to x-ray film (Cytiva). As necessary, after stripping procedure using the Restore Western Blot Stripping Buffer (Thermo Fisher Scientific), membranes were re-probed with primary and secondary antibodies, as previously described [47].

Table 2 Sequences of the primers and probes employed

Primer/probes	Sequence
γ-Globin forward (primer)	5′-TGACAAGCTGCATGTGGATC-3′
γ-Globin reverse (primer)	5′-TTCTTTGCCGAAATGGATTGC-3′
γ-Globin probe	5′-FAM-TCACCAGCACATTTCCCAGGAGC-BFQ-3′
β-Globin forward (primer)	5′-GGTGAATTCTTTGCCAAAGTGAT-3′
β-Globin reverse (primer)	5′-GGGCACCTTTGCCACAC-3′
β-Globin probe	5′-Cy5-ACGTTGCCCAGGAGCCTGAAG-BFQ-3′
α-Globin forward (primer)	5′-GGTCTTGGTGGTGGGGAAG-3′
α-Globin reverse (primer)	5′-CGACAAGACCAACGTCAAGG-3′
α-Globin probe	5′-HEX/ACATCCTCTCCAGGGCCTCCG-BFQ-3′
NF-κB p50 forward (primer)	5′-GGATCTGCACTGTAACTGCT-3′
NF-κB p50 reverse (primer)	5′-CTCTGTCATTCGTGCTTCCA-3′
NF-κB p50 probe	5′-FAM-TGTCACATGAAGTATACCCAGGTTTGCG-BFQ-3′
IL-6 forward (primer)	5′-TTCTGTGCCTGCAGCTTC-3′
IL-6 reverse (primer)	5′-GCAGATGAGTACAAAAGTCCTGA-3′
IL-6 probe	5′-FAM-CAACCACAA ATGCCAGCCAGCCTGCT BFQ-3′
RPL13A forward (primer)	5′-GGCAATTTCTACAGAAACAAGTTG-3′
RPL13A reverse (primer)	5′-GTTTTGTGGGGCAGCATCC-3′
RPL13A probe	5′-HEX-CGCACGGTCCGCCAGAAGAT-BFQ-3′
β-Actin forward (primer)	5′-ACAGAGCCTCGCCTTTG-3′
β-Actin reverse (primer)	5′-ACGATGGAGGGGAAGACG-3′
β-Actin probe	5′-Cy5-CCTTGCACATGCCGGAGCC-BFQ-3′
GAPDH forward (primer)	5′-ACATCGCTCAGACACCATG-3′
GAPDH reverse (primer)	5′-TGTAGTTGAGGTCAATGAAGGG-3′
GAPDH probe	5′-FAM-AAGGTCGGAGTCAACGGATTTGGTC-BFQ-3′
ACE2 forward (primer)	5′-GCCACTGCTCAACTACTTTG-3′
ACE2 reverse (primer)	5′-GCTTATCCTCACTTTGATGCTTTG-3′
ACE2 probe	5′-FAM-ACTCCAGTCGGTACTCCATCCCA-BFQ-3′
SPIKE forward (primer)	5′-CGAGGTGGCCAAGAATCTGA-3′
SPIKE reverse (primer)	5′-TAGGCTAAGCGTTTTGAGCTG-3′

Abbreviations: ACE2=Angiotensin-converting enzyme 2; NF-κB=nuclear factor kappa B; GAPDH=glyceraldehyde-3-phosphate dehydrogenase; FAM = Fluorescein amidite; HEX = Hexachlorofluorescein; BFQ = Binary Fluorescence Quencher.

The quantification of obtained bands was carried out by Chemi-Doc (Bio-Rad), and densitometric analysis was performed using Image Lab Software (Bio-Rad).

Enzyme-Linked Immunosorbent Assays

The presence of S-protein in the culture medium of BNT162b2-treated ErPCs was assessed by using the ELISA kit Human SARS-CoV-2 (COVID-19) Spike Protein S1 Antigen Quantitative ELISA (KRISHGEN BioSystem, cat # KBVH015-10). At the end of the culture the supernatants of the cell cultures were collected and stored at −80°C until analysis. Samples were diluted and analyzed using all the materials provided in the kit following the manufacturer's

instruction manual. The OD was measured at 450 nm using a microplate reader (Tecan Sunrise plate reader) and analyzed using the XFLUOR4 Version: V 4.51 software.

Computational Studies

All the computational methodologies were carried out on a 32 Core AMD Ryzen 93,905 ×, 3.5 GHz Linux Workstation (O.S. Ubuntu 20.04) equipped with Graphics Processing Unit (GPU) (Nvidia Quadro RTX 4000, 8 GB).

The SARS-CoV-2 spike receptor-binding domain (RBD) and HbF structures were retrieved from the Protein Data Bank (PDB-IDs: 7kn5 and 4mqj, respectively). The interaction geometry between the

Table 3 List of primary antibodies used to perform Western blot analysis and their manufacturer names

Target	Primary antibody	Cat. no.
γ-Globin	Rabbit anti-γ-globin (Thermo Fisher Scientific Inc.)	PA5-29006
Transferrin receptor (CD71)	Rabbit anti-TfR (ABclonal)	A22161
β-actin	Rabbit anti-β-actin (Cell Signalling Technology)	4967
SARS-CoV-2 Spike S1	Rabbit anti-spike S1 (GeneTex)	GTX135360

Abbreviations: SARS-CoV-2=Severe acute respiratory syndrome coronavirus 2.

proteins was predicted using the HDOCKlite version 1.0 software [48] generating 100 different poses. To investigate the reliability of the predicted binding geometry, the top-scored complex was submitted to all-atom unbiased molecular dynamics (MDs) simulation using the GROMACS software [49] patched with the open-source, community-developed Plumed ver 2.6.5 [50] under the Charmm36 force field [51]. The complex was included in a rectangular box of $9.2 \times 8.8 \times 12.7$ nm length, solvated and neutralized using 0.15M sodium chloride. The full system containing 100,530 atoms was energy minimized with the steepest descent algorithm, then equilibrated under first constant Number of molecules, Volume and Temperature (NVT) and then constant Number of molecules, Pressure and Temperature (NPT) conditions for 100 and 200 ps, respectively. Long-range electrostatic interactions were modeled using the Particle Mesh Ewald algorithm. LINCS, Nosé−Hoover, and Parrinello−Rahman algorithms were used in the simulations for restraints, and as thermostat and barostat, respectively. MDs were conducted for 25 ns with 2 fs time steps.

To compute the binding energy of the RBD/HbF complex, coarse graining (CG) umbrella sampling (US) simulation was run under the martini v2.2 force field [52]. CG parameters for heme groups were derived from literature [53]. RBD, ACE2, and HbF were converted to the corresponding CG models using the martinize2 script [54]. To preserve the ternary structure of the proteins, the elastic network approach with default parameters was used. Complexes (RBD/ACE2 or RBD/HbF) were included in a box of $20 \times 10 \times 10$ nm length placing the center of geometry (CoG) of ACE2 or HbF at $x=6$, $y=5$, $z=5$ nm, respectively. CG-MDs were conducted with 20 fs time steps. In both cases, the center of CoG of backbone (BB) atoms of RBD was gradually pulled away from the CoG of BB atoms of either ACE2 of HbF using a harmonic restraint with a force constant of 150 kJ/mol·nm^2. Twenty-three equally spaced US windows were then selected for both complexes with CoG−CoG distances ranging from 4.2 to 8.5 nm. Each US window was run for 40 ns restraining the CoG of RBD in place using a force constant of 300 kJ/mol·nm^2. The potential of mean forces (PMF) was then computed according to the WHAM methodology using the wham.py script (http://membrane.urmc.rochester.edu/?page_id=126). PMFs were thus computed by simulating 920 ns for both complexes. One

hundred cycles of Monte Carlo bootstrap analysis were run to determine the error associated with the computation of PMFs.

Statistics

All the data were normally distributed and presented, unless otherwise stated, as mean ± SD. Statistical differences between groups were compared using one-way analyses of variance (ANOVA) between groups software. Statistical differences were considered significant when $p < 0.05$ (*), and highly significant when $p < 0.01$ (**) and $p < 0.001$ (***).

RESULTS

Treatment of CD34$^+$-ErPCs from Patients with β-Thalassemia with SARS-CoV-2 S-Protein and COVID-19 BNT162b2 Vaccine: Effects on Cell Growth

After treatment of *CD34$^+$-ErPCs* with either S-protein or the BNT162b2 vaccine (4−6 days in the presence of EPO), cell number/mL values were determined, to verify possible effects on cell growth. The results obtained demonstrated that all cultures exposed to S-protein did not exhibit any significant decrease of cell number/mL values, suggesting that the treatment with the S-protein does not cause inhibition of the growth rate of treated CD34$^+$-ErPCs (Supplementary Figure E3). On the contrary, when the experiment was carried out with the BNT162b2 vaccine, a slight, but significant reduction of the cell number/mL values was found, suggesting that the treatment of CD34$^+$-ErPCs with the BNT162b2 vaccine causes to some extent inhibition of cell growth (Supplementary Figure E3). These data support the concept that the activity (for instance translation) of the RNA carried by the BNT162b2 vaccine, and/or the delivery material, might interfere with basic processes of treated CD34$^+$-ErPCs.
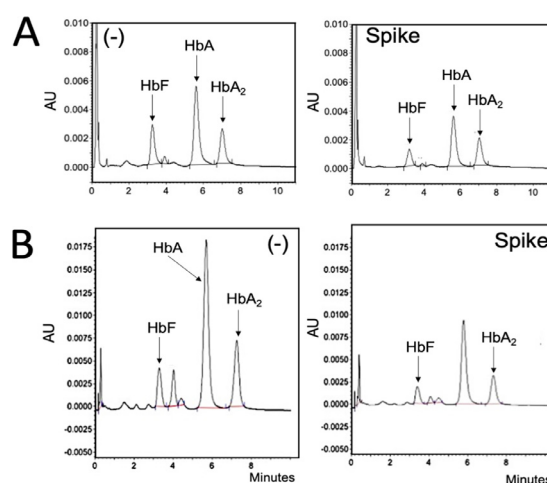
Figure 1 Effects of spike exposure on hemoglobin accumulation. ErPCs from patients #1 **(A)**, and #2 **(B)** were either untreated (cultured with only EPO) (-), or exposed to 20 nM SARS-CoV-2 S-protein (right side of the **A** and **B** panels) before culturing with EPO. Lysates from the same number of cells were analyzed. ErPC=Erythroid precursor cells; EPO=erythropoietin; SARS-CoV-2 S-protein= severe acute respiratory syndrome coronavirus 2 spike protein.
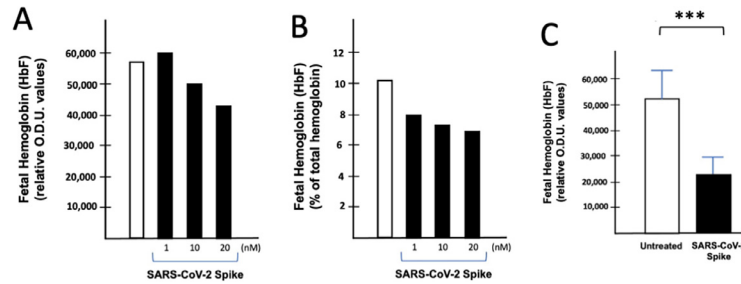
Figure 2 Effects of spike exposure on hemoglobin production by treated ErPCs. ErPCs from patients #2 **(A, B)**, were either untreated (cultured with only EPO)(open boxes), or exposed to different concentrations of the SARS-CoV-2 S-protein before culturing with EPO (black boxes). HbF content is presented as relative O.D.U. values (total area of the HbF peaks analyzed by HPLC) **(A)** or as % of total hemoglobin **(B)**. C. Summary of 9 independent experiments (using ErPCs isolated from 5 patients with β-thalassemia) showing a significant decrease of HbF in ErPCs exposed to SARS-CoV-2 Spike protein. The data represent the average $\pm$ SD. ErPC=Erythroid precursor cells; EPO=erythropoietin; HbF=fetal hemoglobin; HPLC=high-performance liquid chromatography; SARS-CoV-2 S-protein= severe acute respiratory syndrome coronavirus 2 spike protein; O.D.U. = optical density unit.

Exposure to SARS-CoV-2 Spike is Associated with a Decrease of HbF Production by ErPCs from Patients with β-Thalassemia

Figure 1 shows representative HPLC results obtained using ErPCs from 2 patients (#1 and #2, see Table 1 for genotypes). These 2 patients have been selected considering that their genotype (β^{+}-IVS1-110/β^{+}-IVS1-110 or β^{0}39/β^{+}-IVS1-110) is compatible with the production of both fetal hemoglobin (HbF) and adult hemoglobin (HbA) (see the HPLC patterns shown in Figure 1), allowing to compare S-protein-mediated inhibitory effects of HbF accumulation with the effects on HbA production. As shown in Figure 1, the ErPCs employed exhibited different starting levels of fetal hemoglobin, in agreement with previous observations suggesting that this biochemical parameter (HbF production) is highly variable in patients with β-thalassemia [34]. The results obtained indicate the production of HbF, HbA, and HbA2 in the EPO-induced cultures. Exposure to SARS-CoV-2 S-protein (20 nM; right side of the panels) caused in all the experiments a decrease of total hemoglobin production; the decrease was particularly evident when HbF was analyzed (54.04% and 53.3% decrease of HbF in S-protein-treated
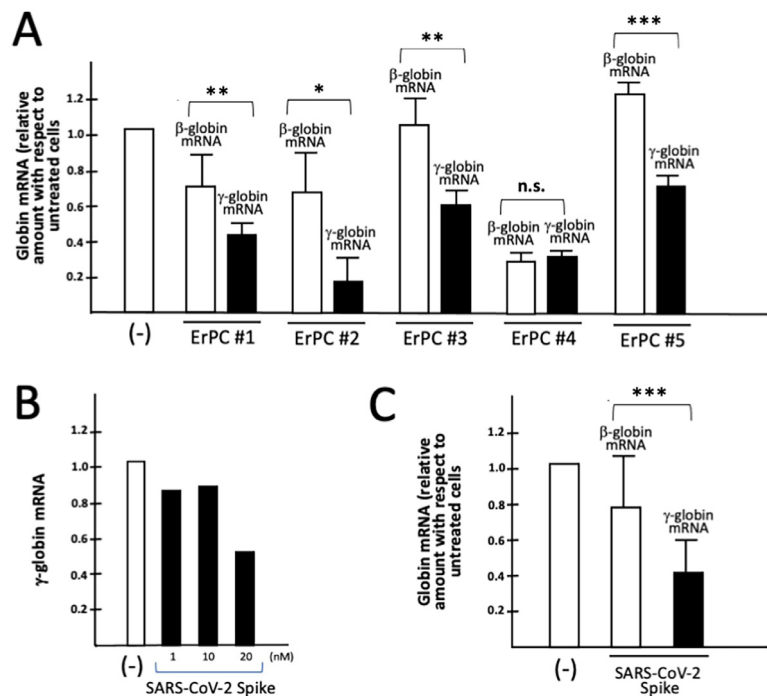
Figure 3 Effects of exposure to SARS-CoV-2 S-protein: globin gene expression in treated ErPCs. **(A)** ErPCs from patients #1, #2, #3, #4, and #5 (ErPC #1, #2, #3, #4, and #5 as indicated) were either untreated (cultured with only EPO), or exposed to SARS-CoV-2 spike protein before culturing with EPO. The relative amount of β-globin (white boxes) and γ-globin (black boxes) mRNA have been evaluated by RT-qPCR. **(B)** RT-qPCR analysis of γ-globin mRNA in ErPC #2, either untreated or exposed to increasing concentrations of the SARS-CoV-2 spike protein. **(C)** Summary of the independent experiments conducted using S-protein—exposed ErPCs. The data of panels **A** and **C** represent the average $\pm$ S.D (n = 3 and 9, respectively). ErPC=Erythroid precursor cells; EPO=erythropoietin; RT-qPCR= real-time reverse-transcription PCR; SARS-CoV-2 S-protein= severe acute respiratory syndrome coronavirus 2 spike protein.
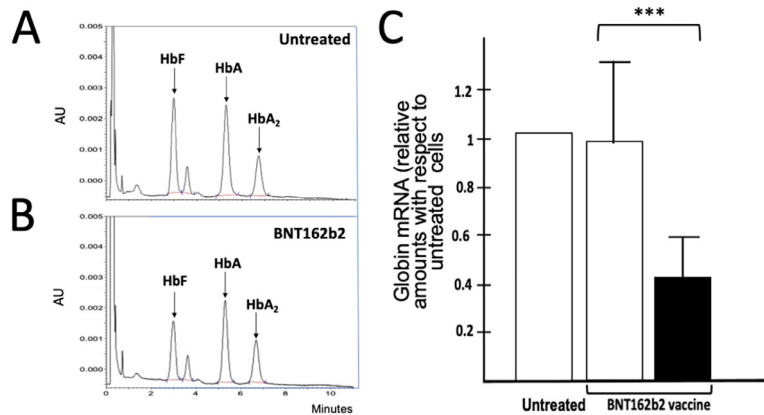
Figure 4 Effects of the BTN162b2 vaccine on hemoglobin accumulation and globin gene expression by treated ErPCs. **(A, B)** Effects on hemoglobin accumulation. ErPCs from patient #1 were either untreated (cultured with only EPO) **(A)** or exposed to the COVID-19 BTN162b2 vaccine before culturing with EPO **(B)**. The resulting HPLC patterns are shown. **(C)** Summary of the results obtained analyzing the accumulation of β-globin (white box) and γ-globin (black box) mRNAs in ErPCs from all the recruited patients treated with the COVID-19 BTN162b2 vaccine. The data represent the average ± SD. ErPC=Erythroid precursor cells; EPO=erythropoietin; HPLC= high-performance liquid chromatography.

ErPCs from patient #1 and #2, respectively: panels A and B of Figure 1).

The effect of spike is dose-dependent as suggested by the experiment shown in Figure 2. The overall decrease (Figure 2A) in total hemoglobin and the decrease in the % of HbF with respect to total hemoglobin (Figure 2B) is evident with 20 nM spike concentration, taking into consideration that the lysates from the same number of ErPCs were always loaded on the HPLC column. After this preliminary experiment, to extend the analysis, 5 EPO-treated ErPC cultures were exposed to S-protein for 6 days, and then HbF was quantified and compared with control EPO-treated cultures not exposed to S-protein. The results obtained demonstrate that the decrease in HbF production in S-protein-treated ErPCs is reproducible (Fig. 2C). To further verify these data, the expression of γ-globin genes was determined, because it is known that the expression of γ-globin genes is strongly correlated with HbF ($\alpha_2\gamma_2$) accumulation [34,35].

The SARS-CoV-2-Mediated Decrease of Hemoglobin Production by ErPCs is Associated with Impairment of the Erythropoietin-Mediated Expression of Globin Genes

Figure 3A shows that there was a significant ($p < 0.05$) decrease of γ-globin mRNA in the spike-treated ErPCs from the 5 patients with β-thalassemia. Interestingly, and fully in agreement with the HPLC data, the extent of the γ-globin mRNA decrease is higher than the extent of the β-globin mRNA decrease, supporting the observed decrease of the percentage of HbF with respect to the total hemoglobin production in SARS-CoV-2 S-protein-treated ErPCs (Figures 1 and 2). The S-protein-mediated inhibition of γ-globin gene expression is dose-dependent (Figure 3B) and highly reproducible (Figure 3C).

Effects of the BNT162b2 Vaccine on EPO-Mediated Induction of Globin Genes: Evidence for Preferential Effects on HbF Production and Expression of γ-Globin Genes

Panels A and B of Figure 4 show HPLC results obtained using ErPCs from patient #1, either untreated (Figure 4A) or treated with 1 μg/mL BNT162b2 (Figure 4B). As clearly evident, the HbF peak is

decreased both considering absolute HPLC values (from 43,383 to 27,570, considering the areas of the HbF peaks in panels A and B, respectively) and values relative to the other hemoglobin peaks (% with respect to total hemoglobin production: from 34.6% in untreated cells to 27.5% in BNT162b2-treated cells). This decrease in HbF production (HPLC analysis) in BNT162b2-treated cells was confirmed by the RT-qPCR data shown in Figure 4C, which indicates a preferential decrease in the accumulation of γ-globin mRNA in the BNT162b2-treated ErPCs.

To verify whether the inhibitory effects of the S-protein affect all the erythroid-associated proteins, including markers of erythroid maturation, the content of γ-globin and the content of transferrin receptor (TrfR) were comparatively analyzed by Western blotting using an antibody recognizing β-actin as an internal control. Representative data are presented in the Supplementary Figure E4A and show that in the ErPC cultures from patient #1 the γ-globin is decreased (fully in agreement with the HPLC data shown in Figure 1A) following treatment of the cells with the S-protein. Quantitative data are shown in Supplementary Figure E4B. By sharp contrast, the content of TrfR does not decrease (Supplementary Figure E4A, B), suggesting that the cell maturation was not impaired by the treatment.

Exposure of ErPCs from Patients with β-Thalassemia to SARS-CoV-2 Spike (S-protein) and BNT162b2 Vaccine is Associated with Activation of Pro-inflammatory Genes

To verify possible effects of S-protein and COVID-19 BNT162b2 vaccine on pro-inflammatory genes, we first analyzed the effects on transcription of nuclear factor kappa B (*NF-κB*) and *IL-6* genes, encoding a key transcription factor (NF-κB) regulating the expression of pro-inflammatory genes [55−57] and a cytokine (IL-6) involved in several inflammatory responses [46] and "COVID-19" cytokine storm" [58,59]. Moreover, IL-6 is also highly present in the plasma of patients with β-thalassemia, as reported by Walter et al. [60] and Vinchi et al. [61]. Figure 5A shows representative RT-qPCR data demonstrating that, in ErPCs from patient #3, the treatment with the SARS-
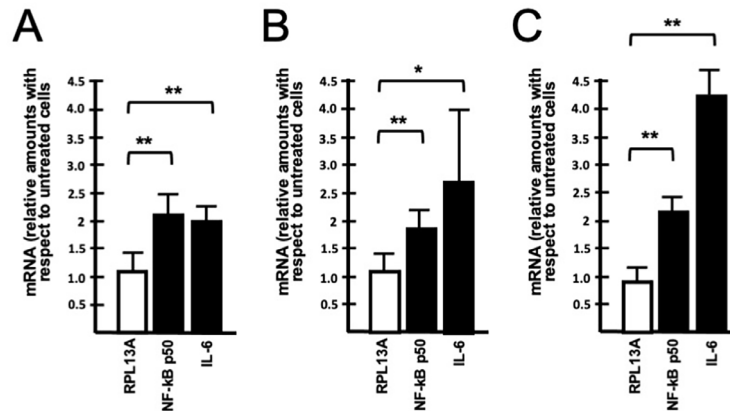
Figure 5 Expression of selected pro-inflammatory genes by ErPCs treated with SARS-CoV-2 S-protein or COVID-19 BNT162b2 vaccine. **(A, B)** Effects of treatment with S-protein on ErPCs from patient #3 (**A**, *n* = 3) or all patients (**B**, *n* = 7) on the accumulation of the ribosomal *RPL13A*, *NF-κB* p50, and *IL-6* mRNAs, as indicated. **(C)** Effects of treatment with the COVID-19 BNT162b2 vaccine. ErPCs were either untreated (cultured with only EPO) (white boxes) or exposed to 25 ng/mL of the SARS-CoV-2 Spike protein or 1 μg/mL of the COVID-19 BNT162b2 vaccine before culturing with EPO (black boxes). The data represent the average ± S.D (n=3). ErPC=Erythroid precursor cells; EPO=erythropoietin; NF-κB, nuclear factor kappa B; SARS-CoV-2 S-protein=severe acute respiratory syndrome coronavirus 2 spike protein.
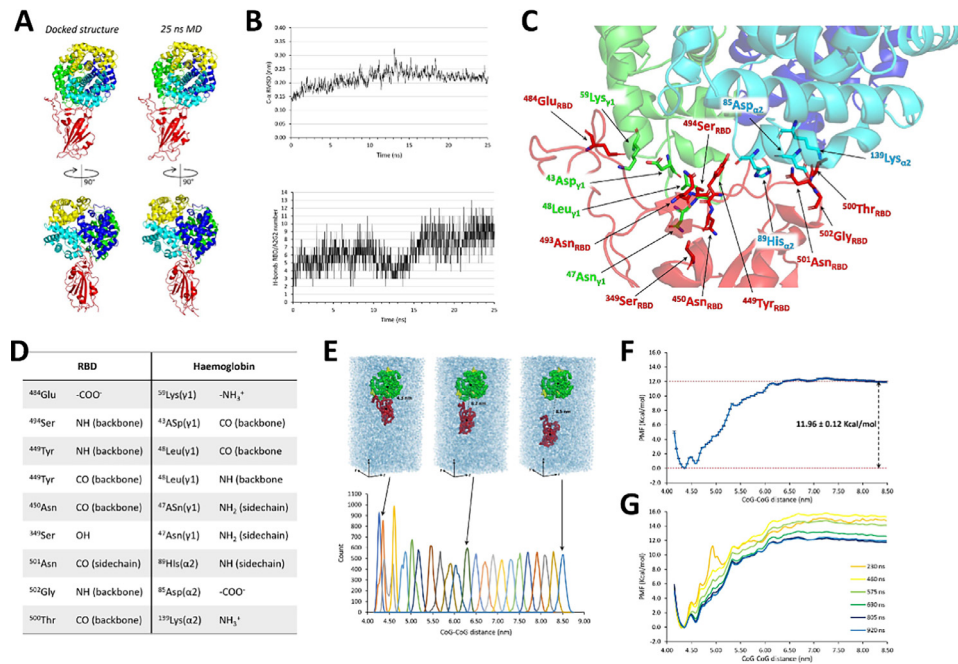
Figure 6 In silico molecular interactions between SARS-CoV-2 S-protein and HbF. **(A)** results of RBD/HbF docking simulation (left) and of 25 ns of MDs (right). RBD is reported as a red cartoon. HbF is reported as blue (alfa1), cyan (alfa2), green (gamma1), and yellow (gamma2) cartoon. **(B)** RMSD (nm) of alfa-carbon atoms (top) and number of H-bonds formed between HbF and RBD (bottom) as a function of MDs simulation time. **(C)** Residues involved in H-bonds between HbF and RBD. Proteins are colored as in panel **A. (D)** A detailed list of H-bond pairs between HbF and RBD. **(E)** Depiction of the first, intermediate, and last forced unbinding event (top) used for the US simulation. The bottom panel shows the sampling distribution within the 23 US windows. **(F)** Free energy profile (kcal/mol) along the reaction coordinate (distance between the CoG of RBD and the CoG of HbF; nm). **(G)** Assessment of convergence of the US simulation. The energy profiles are reported as a function of the total simulation time. CoG=center of geometry; ErPC=erythroid precursor cells; EPO=erythropoietin; HbF=fetal hemoglobin; MDs=molecular dynamics; RBD=receptor-binding domain; RMSD=root-mean squared deviation; US=umbrella sampling.

CoV-2 S-protein induces an increase of *NF-κB*, p50, and *IL-6* mRNA accumulation, in agreement with several reports outlining spike-induced alteration of the expression of pro-inflammatory genes [38,39,46,47].

This was confirmed by analyzing the data obtained in ErPC cultures from all the patients outlined in Table 1. These results are shown in Figure 5B, which demonstrates a significant activation of *NF-κB* and *IL-6* gene expression in spike-treated ErPCs. This part of the study concludes that the SARS-CoV-2 S-protein can cause significant changes in the expression of pro-inflammatory genes in treated ErPCs.

Similarly, also the analysis of ErPCs cells treated with COVID-19 BNT162b2 vaccine shows a significant activation of NF-κB and IL-6 gene expression. The data reported in Figure 5C demonstrate, respectively, a significant increase in activation of *NF-κB* and *IL-6* gene expression compared with the untreated sample.

The SARS-CoV-2 S-Protein Efficiently Interacts with HbF: A Molecular Docking Analysis

We simulated the interaction between HbF and the S-protein RBD using the well-known protein−protein docking software HDOCK [48], obtaining the results shown in Figure 6A, left). The top-scored complex was submitted to 25 ns of all-atom MDs simulation (Figure 6A, right). After the first 10 ns of simulation, during which a slight adjustment of the interaction geometry was noted, the complex resulted almost stable as shown by the Cα-RMSD (Figure 6B, top) with the number of H-bonds between the RBD and HbF increasing from ∼6 to ∼9 (Figure 6B, bottom). Figure 6C shows the residues involved in the interaction between the S-protein RBD and HbF, whereas Figure 6D shows a detailed list of such interactions. Of note, both α-globin and γ-globin HbF subunits were involved in the interaction with SARS-CoV-2 spike RBD. To determine the strength of the interaction, the system was further submitted to US studies. Accordingly, to preliminary assess whether the Martini model was able to correctly predict the binding energy, we first computed the (un)binding free energy between the ACE2 and the RBD through US simulations under their CG representation. Remarkably, the computed interaction energy (12.00 ± 0.35 kcal/mol; not shown) was in line with that computed by all-atom simulations (11.75 kcal/mol) [54], demonstrating that the Martini CG force field can be efficiently used to compute the RBD/HbF interaction energy.

Figure 6E (top) shows the first, one intermediate, and the last US windows, along with the distribution of the sampled CoG−CoG distances after 40 ns of simulations per window (bottom). As can be seen, the simulation time allowed a complete overlapping of the US windows, which is fundamental for the WHAM algorithm to properly compute the PMF. Figure 6F shows the computed energy profile for the dissociation of the complex RBD/HbF. The estimated unbinding energy was 11.96 kcal/mol, which was almost comparable to that computed for the RBD/ACE2 interaction. As can be seen in Figure 6G, the simulation was long enough to ensure the convergence, as the energy profile did not substantially change between 805 (35 ns per US window) and 920 ns (40 ns per US window).

DISCUSSION

The main conclusions of the results reported in the present study are that the SARS-CoV-2 S-protein and the BNT162b2 vaccine (a)

inhibit HbF production by ErPCs from patients with β-thalassemia (Figures 1, 2, and 4A) and (b) inhibit γ-globin mRNA accumulation (Figures 3 and 4C). In addition, we provide in silico studies suggesting a high affinity of SARS-CoV-2 S-protein to fetal hemoglobin. Remarkably, this affinity approaches the affinity of spike to ACE2 (Figure 6).

Our results are consistent with the hypothesis of a relevant impact of SARS-CoV-2 infection and COVID-19 vaccination on the hematopoietic system, as also suggested by several studies recently published by other research groups [4,6,7,24,25].

Based on this conclusion, several considerations should be made. The relevance of determining the effects of spike on mammalian cells (including ErPCs here studied) is related to the fact that spike has been detected by several studies in the bloodstream following SARS-CoV-2 infection or vaccination. For instance, a study published in May 2021 documented, for the first time, circulating vaccine-induced S-protein in the blood as early as one day after injection [23,58]. Although in this study the concentrations reached were several orders of magnitude lower than those needed to bind ACE2 receptors [58], a further report has been published describing the case of a woman suffering from Moderna-COVID-19-vaccine−induced thrombocytopenia and with 10 ng/mL vaccine-induced S-protein levels in plasma 10 days after vaccination (∼100 times higher than those reported previously), suggesting excessive vaccine-induced production of S-protein as a determinant of vaccine toxicity [23,59]. The data available suggest that, after vaccination with both Moderna or BioNTech −Pfizer COVID-19 vaccines, endogenous production of S-protein following vaccination may occur for much longer than previously thought [11].

Interestingly, S-protein has been suggested as responsible for toxicity of COVID-19 vaccines by several studies [11−14]. For example, Yonker et al. [14] recently reported the detection of markedly elevated levels of full-length S-protein, unbound by antibodies, in the plasma of individuals with postvaccine myocarditis. Interestingly, no free spike was detected in asymptomatic vaccinated control subjects [14]. This and similar studies have stimulated research projects aimed to determine the possible effects of SARS-CoV-2 infection and/or COVID-19 vaccination on selected biological functions and tissue systems. In this respect, Estep et al. [32] have evaluated the effects of SARS-CoV-2 infection and/or COVID-19 vaccination of mothers on the fate and functionalities of HSPCs in the umbilical cord blood (UCB). The numbers and frequencies of HSPCs in the UCB decreased significantly in donors with previous SARS-CoV-2 infection and, importantly, with COVID-19 vaccination via the induction of apoptosis, likely mediated by IFN-γ-dependent pathways. These results indicate that SARS-CoV-2 infection and COVID-19 vaccination impair the functionalities and survivability of HSPCs in the UCB, which would make unprecedented concerns on the future of cellular therapies based on hematopoietic cells exhibiting an altered phenotype following SARS-CoV-2 infection and/or COVID-19 vaccination [27]. The possible impact of SARS-CoV-2 infection and COVID-19 vaccination on the hematopoietic system has been confirmed by other studies [6,7,24,25]. For instance, Ropa et al. [24] found that SARS-CoV-2 S-protein inhibits the expansion of hematopoietic stem/progenitor cells and deeply alters colony-forming capacity. These effects were obtained by a simple exposure to S-protein, even in the absence of a true SARS-CoV-2 infection.

Concerning the molecular basis of S-protein−mediated effects on the accumulation of γ-globin mRNA, a possible explanation is spike-

mediated alterations of transcription factors, such as NF-κB, which are known to be induced by S-protein [22,48,62]. Interestingly, NF-κB is known to suppress the expression of erythroid genes, including globin genes [63]. Accordingly, induction of NF-κB (for instance by IFN-γ) is associated with inhibition of expression of γ-globin genes. For instance, Lee et al. [64] found that IFN-γ modulates NF-κB/c-Jun to antagonize activin A-mediated NF-E2 transcriptional activity on globin gene expression. Accordingly, NF-κB inhibitors (such as trimethyl angelicin) [65] are also powerful inducers of γ-globin gene expression and HbF production [66].

Our study supports the conclusion of several other reports suggesting clinical hematologic relevance of SARS-CoV-2 infection and vaccination. In this respect, a very important issue is the possible occurrence of alteration of hematologic parameters during PASC. Accordingly, our study supports the concept that during PASC (but also after vaccination) hematologic parameters should be monitored, especially in the case circulating S-protein is maintained at high levels. This might be relevant, in our opinion, in the case of subjects affected by hemoglobinopathies (such as β-thalassemia and sickle-cell disease) who can have important beneficial effects in the case HbF is highly produced. A strong consensus does exist on the fact that in β-thalassemia and SCD the HbF levels are intimately associated with the severity of the disease [33]. Our data suggest that the effects of COVID-19 vaccination should be carefully monitored in patients with β-thalassemia. In this respect, the comparison of clinical trials executed on patients with β-thalassemia before and after the COVID-19 pandemic might be of great interest. For instance, the Sir-thalaclin (NCT03877809) and Thala-Rap (NCT04247750) clinical trials (using low dosages of rapamycin/sirolimus for HbF induction) were conducted before the COVID-19 pandemic (the NCT03877809 trial) or during the COVID-19 pandemic (the NCT04247750 trial). In this latter case, the clinical trial has been conducted on patients who have been vaccinated at the beginning of the treatment. The comparison of the data regarding globin mRNA expression and hemoglobin production in the NCT04247750 trial might be of top interest when compared with the already reported data from the NCT03877809 trial [34].

According to previous studies that suggested a binding between spike and hemoglobin [67], HbF was supposed to directly interact with the RBD. Here we have combined docking and molecular dynamics simulation to further reinforce the hypothesis that HbF can bind the RBD. The computed free energy of (un)binding (11.96 kcal/mol) is comparable to that of RBD/ACE2 (12.00 kcal/mol), suggesting that the S-protein interacts with HbF with the same efficiency exhibited in the interactions with ACE2.

Our results encourage analysis of the effects on erythroid precursors/progenitors in patients with β-thalassemia after vaccination with both Moderna and BioNTech−Pfizer COVID-19 vaccines, as well as a careful analysis of HbF production in patients with SARS-CoV-2−infected COVID-19 β-thalassemia. Our study suggests that pharmacologic strategies should be considered to solve hematopoiesis-associated alterations due to SARS-CoV-2 infection and/or COVID-19 vaccination. Focusing on HbF production, the reversion of S-protein-mediated HbF inhibition can be achieved, at least in theory, by using HbF inducers, such as hydroxyurea [68] and sirolimus [34].

A limitation of our study is the employment of only one type of SARS-CoV-2 (the original S-protein) and only one RNA-based vaccine (the BNT162b2 vaccine from Pfizer/Biontech). As far as the first issue, it is well known that various mutants of SARS-CoV-2 arrived,

mainly concerned with the S-protein. Although this has a clear impact on the design of novel updated and effective vaccines, further studies should be designed to determine the impact of these mutations with respect to the bioactivity of the S-protein, including the inhibitory effects on globin gene expression described in the present study. In this respect, the impact of S-protein mutations on structure and functions has been recognized [69−73].

As far as the second issue, a more extensive study is needed comparing the BNT162b2 vaccine with all other available COVID-19 RNA-based vaccines (both those approved and those under clinical trials), such as mRNA-1273, mRNA-1273.351, and mRNA-1273.211 (Moderna TX, Inc.), CVnCoV (Cure Vac), ARCoV (AMS, Walvax Biotechnology and Suzhou Abogen Bio-Sciences), and ARCT-154 (Arcturus Therapeutic) [74].

A further limitation of our study is that the expression of a few genes has been analyzed. In this respect, "omics" analyses are expected to be important for understating the real impact of treatments with S-protein and RNA-based COVID-19 vaccines on the overall gene expression of CD34^{+}-ErPCs. As far as the analysis of markers of erythroid maturation, in addition to transferrin receptor, other proteins should be studied, including glycophorin A, spectrin, proteins involved in the heme biosynthesis, and others.

In conclusion, our ex vivo study suggests that the SARS-CoV-2 S-protein and COVID-19 vaccine retain inhibitory effects on hemoglobin production by ErPCs isolated from patients with β-thalassemia. Further in vivo studies are warranted using primary cells from healthy people as well as cells from subjects affected by other hemoglobinopathies (such as sickle-cell disease) or patients with β-thalassemia carrying genotypes different from those considered in the present study.

Conflict of Interest Disclosure

The authors do not have any conflicts of interest to declare in relation to this work.

Author Contributions

RG, AF, and GM conceived and designed the work and wrote the manuscript. GM was responsible for the molecular docking and molecular dynamics experiments. LCC, JG, MZ, and CZ performed the experiments and analyzed and interpreted the data. RG, GM, and AF were responsible for funding acquisition. All authors read and approved the final manuscript.

Data Availability

All the data concerning this study are present within the main text and Supplementary materials. Additional information will be freely available upon reasonable request to the corresponding author.

Funding

Ethics Approval and Consent to Participate

The study was conducted according to the guidelines of the Declaration of Helsinki, and the use of human material was approved by the Ethics Committee of Ferrara's District, protocol name: THAL-THER, document number 533/2018/Sper/AOUFe, approved on 14 November 2018. All samples of peripheral blood were obtained after receiving written informed consent from donor patients or their legal representatives.

SUPPLEMENTARY MATERIALS

Supplementary material associated with this article can be found in the online version at https://doi.org/10.1016/j.exphem.2023.11.002.

REFERENCES

1. Chen G, Wu D, Guo W, et al. Clinical and immunological features of severe and moderate coronavirus disease 2019. J Clin Invest 2020;130:2620–9. https://doi.org/10.1172/JCI137244.
2. Wang C, Horby PW, Hayden FG, Gao GF. A novel coronavirus outbreak of global health concern. Lancet 2020;395:470–3. https://doi.org/10.1016/S0140-6736(20)30185-9.
3. Jia S, Li Y, Fang T. System dynamics analysis of COVID-19 prevention and control strategies. Environ Sci Pollut Res Int 2021;29:3944–57. https://doi.org/10.1007/s11356-020-11060-z.
4. Elahi S. Hematopoietic responses to SARS-CoV-2 infection. Cell Mol Life Sci 2022;79:187. https://doi.org/10.1007/s00018-022-04220-6.
5. Allahyani MA, Aljuaid AA, Almehmadi MM, et al. Detection of erythroid progenitors and erythrocytopathies in patients with severe COVID-19 disease. Saudi Med J 2022;43:899–906. https://doi.org/10.15537/smj.2022.43.8.20220311.
6. Kronstein-Wiedemann R, Stadtmüller M, Traikov S, et al. SARS-CoV-2 infects red blood cell progenitors and dysregulates hemoglobin and iron metabolism. Stem Cell Rev Rep 2022;18:1809–21. https://doi.org/10.1007/s12015-021-10322-8.
7. Encabo HH, Grey W, Garcia-Albornoz M, et al. Human erythroid progenitors are directly infected by SARS-CoV-2: implications for emerging erythropoiesis in severe COVID-19 patients. Stem Cell Rep 2021;16:428–36. https://doi.org/10.1016/j.stemcr.2021.02.001.
8. Watson OJ, Barnsley G, Toor J, Hogan AB, Winskill P, Ghani AC. Global impact of the first year of COVID-19 vaccination: a mathematical modelling study. Lancet Infect Dis 2022;22:1293–302. https://doi.org/10.1016/S1473-3099(22)00320-6.
9. World Health Organization (WHO). Emergency Committee regarding the coronavirus disease (COVID-19) pandemic. 30 January 2023. Statement on the fourteenth meeting of the International Health Regulations; 2005.
10. Kouhpayeh H, Ansari H. Adverse events following COVID-19 vaccination: a systematic review and meta-analysis. Int Immunopharmacol 2022;109:108906. https://doi.org/10.1016/j.intimp.2022.108906.
11. Frasca L. Safety of COVID-19 vaccines in patients with autoimmune diseases, in patients with cardiac issues, and in the healthy population. Pathogens 2023;12:233. https://doi.org/10.3390/pathogens12020233.
12. Trougakos IP, Terpos E, Alexopoulos H, et al. Adverse effects of COVID-19 mRNA vaccines: the spike hypothesis. Trends Mol Med 2022;28:542–54. https://doi.org/10.1016/j.molmed.2022.04.007.
13. Cosentino M, Marino F. The spike hypothesis in vaccine-induced adverse effects: questions and answers. Trends Mol Med 2022;28:797–9. https://doi.org/10.1016/j.molmed.2022.07.009.
14. Yonker LM, Swank Z, Bartsch YC, et al. Circulating spike protein detected in post-COVID-19 mRNA vaccine myocarditis. Circulation 2023;147:867–76. https://doi.org/10.1161/CIRCULATIONAHA.122.061025.
15. Talotta R. Impaired VEGF-A-mediated neurovascular crosstalk induced by SARS-CoV-2 spike protein: a potential hypothesis explaining long COVID-19 symptoms and COVID-19 vaccine side effects? Microorganisms 2022;10:2452. https://doi.org/10.3390/microorganisms10122452.
16. Ogata AF, Cheng CA, Desjardins M, et al. Circulating severe acute respiratory syndrome coronavirus 2 (SARS-CoV-2) vaccine antigen detected in the plasma of mRNA-1273 vaccine recipients. Clin Infect Dis 2022;74:715–8. https://doi.org/10.1093/cid/ciab465.
17. Sahin U, Muik A, Vogler I, et al. BNT162b2 vaccine induces neutralizing antibodies and poly-specific T cells in humans. Nature 2021;595:572–7. https://doi.org/10.1038/s41586-021-03653-6.
18. Bansal S, Perincheri S, Fleming T, et al. Cutting edge: circulating exosomes with COVID spike protein are induced by BNT162b2 (Pfizer-BioNTech) vaccination prior to development of antibodies: a novel mechanism for immune activation by mRNA vaccines. J Immunol 2021;207:2405–10. https://doi.org/10.4049/jimmunol.2100637.
19. Pegu A, O'Connell SE, Schmidt SD, et al. Durability of mRNA-1273 vaccine-induced antibodies against SARS-CoV-2 variants. Science 2021;373:1372–7. https://doi.org/10.1126/science.abj4176.
20. Huang X, Huang B, He Y, et al. SARS-CoV-2 spike protein-induced damage of hiPSC-derived cardiomyocytes. Adv Biol (Weinh) 2022;6:e2101327. https://doi.org/10.1002/adbi.202101327.
21. Avolio E, Carrabba M, Milligan R, et al. The SARS-CoV-2 spike protein disrupts human cardiac pericytes function through CD147 receptor-mediated signalling: a potential non-infective mechanism of COVID-19 microvascular disease. Clin Sci (Lond) 2021;135:2667–89. https://doi.org/10.1042/CS20210735.
22. Robles JP, Zamora M, Adan-Castro E, Siqueiros-Marquez L, Martinez de la Escalera G, Clapp C. The spike protein of SARS-CoV-2 induces endothelial inflammation through integrin $\alpha5\beta1$ and NF-κB signaling. J Biol Chem 2022;298:101695. https://doi.org/10.1016/j.jbc.2022.101695.
23. Lei Y, Zhang J, Schiavon CR, et al. SARS-CoV-2 spike protein impairs endothelial function via downregulation of ACE 2. Circ Res 2021;128:1323–6. https://doi.org/10.1161/CIRCRESAHA.121.318902.
24. Ropa J, Cooper S, Capitano ML, Van't Hof W, Broxmeyer HE. Human hematopoietic stem, progenitor, and immune cells respond ex vivo to SARS-CoV-2 spike protein. Stem Cell Rev Rep 2021;17:253–65. https://doi.org/10.1007/s12015-020-10056-z.
25. Kucia M, Ratajczak J, Bujko K, et al. An evidence that SARS-CoV-2/COVID-19 spike protein (SP) damages hematopoietic stem/progenitor cells in the mechanism of pyroptosis in Nlrp3 inflammasome-dependent manner. Leukemia 2021;35:3026–9. https://doi.org/10.1038/s41375-021-01332-z.
26. Lee KM, Lin SJ, Wu CJ, Kuo RL. Race with virus evolution: the development and application of mRNA vaccines against SARS-CoV-2. Biomed J 2023;46:70–80. https://doi.org/10.1016/j.bj.2023.01.002.

27. Cosentino M, Marino F. Understanding the pharmacology of COVID-19 mRNA vaccines: playing dice with the spike? Int J Mol Sci 2022;23:10881. https://doi.org/10.3390/ijms231810881.

28. Bellavite P, Ferraresi A, Isidoro C. Immune Response and Molecular Mechanisms of Cardiovascular Adverse Effects of Spike Proteins from SARS-CoV-2 and mRNA Vaccines. Biomedicines 2023; 11:451. https://doi.org/10.3390/biomedicines11020451.

29. Swank Z, Senussi Y, Manickas-Hill Z, et al. Persistent circulating severe acute respiratory syndrome coronavirus 2 spike is associated with post-acute coronavirus disease 2019 sequelae. Clin Infect Dis 2023;76:e487–90. https://doi.org/10.1101/2022.06.14.22276401.

30. Craddock V, Mahajan A, Spikes L, et al. Persistent circulation of soluble and extracellular vesicle-linked spike protein in individuals with postacute sequelae of COVID-19. J Med Virol 2023;95:e28568. https://doi.org/10.1002/jmv.28568.

31. Schultheiß C, Willscher E, Paschold L, et al. Liquid biomarkers of macrophage dysregulation and circulating spike protein illustrate the biological heterogeneity in patients with post-acute sequelae of COVID-19. J Med Virol 2023;95:e28364. https://doi.org/10.1002/jmv.28364.

32. Estep BK, Kuhlmann CJ, Osuka S, et al. Skewed fate and hematopoiesis of CD34+ HSPCs in umbilical cord blood amid the COVID-19 pandemic. iScience 2022;25:105544. https://doi.org/10.1016/j.isci.2022.105544.

33. Fibach E, Bianchi N, Borgatti M, Prus E, Gambari R. Mithramycin induces fetal hemoglobin production in normal and thalassemic human erythroid precursor cells. Blood 2003;102:1276–81. https://doi.org/10.1182/blood-2002-10-3096.

34. Zuccato C, Cosenza LC, Zurlo M, et al. Expression of γ-globin genes in β-thalassemia patients treated with sirolimus: results from a pilot clinical trial (Sirthalaclin). Ther Adv Hematol 2022;13:20406207221100648. https://doi.org/10.1177/20406207221100648.

35. Zuccato C, Cosenza LC, Zurlo M, et al. Treatment of erythroid precursor cells from β-thalassemia patients with cinchona alkaloids: induction of fetal hemoglobin production. Int J Mol Sci 2021;22:13433. https://doi.org/10.3390/ijms222413433.

36. Cosenza LC, Breda L, Breveglieri G, et al. A validated cellular biobank for β-thalassemia. J Transl Med 2016;14:255. https://doi.org/10.1186/s12967-016-1016-4.

37. Wang W, Ye L, Ye L, et al. Up-regulation of IL-6 and TNF-alpha induced by SARS-coronavirus spike protein in murine macrophages via NF-κB pathway. Virus Res 2007;128:1–8. https://doi.org/10.1016/j.virusres.2007.02.007.

38. Gasparello J, d'Aversa E, Breveglieri G, Borgatti M, Finotti A, Gambari R. In vitro induction of interleukin-8 by SARS-CoV-2 spike protein is inhibited in bronchial epithelial IB3-1 cells by a miR-93-5p agomiR. Int Immunopharmacol 2021;101:108201. https://doi.org/10.1016/j.intimp.2021.108201.

39. Gasparello J, D'Aversa E, Papi C, et al. Sulforaphane inhibits the expression of interleukin-6 and interleukin-8 induced in bronchial epithelial IB3-1 cells by exposure to the SARS-CoV-2 spike protein. Phytomedicine 2021;87:153583. https://doi.org/10.1016/j.phymed.2021.153583.

40. Cavezzi A, Troiani E, Corrao S. COVID-19: hemoglobin, iron, and hypoxia beyond inflammation. A narrative review. Clin Pract 2020;10:1271.

41. Shahbaz S, Xu L, Osman M, et al. Erythroid precursors and progenitors suppress adaptive immunity and get invaded by SARS-CoV-2. Stem Cell Rep 2021;16:1165–81. https://doi.org/10.1016/j.stemcr.2021.04.001.

42. Wang K, Chen W, Zhang Z, et al. CD147-spike protein is a novel route for SARS-CoV-2 infection to host cells. Signal Transduct Target Ther 2020;5:283. https://doi.org/10.1038/s41392-020-00426-x.

43. Zhou YQ, Wang K, Wang XY, Cui HY, Zhao Y, Zhu P, Chen ZN. SARS-CoV-2 pseudovirus enters the host cells through spike protein-CD147 in an Arf6-dependent manner. Emerg Microbes Infect 2022;11:1135–44. https://doi.org/10.1080/22221751.2022.2059403.

44. Zhang GF, Meng W, Chen L, et al. Infectivity of pseudotyped SARS-CoV-2 variants of concern in different human cell types and inhibitory effects of recombinant spike protein and entry-related cellular factors. J Med Virol 2023;95:e28437. https://doi.org/10.1002/jmv.28437.

45. Li Y, Zhang Z, Yang L, et al. The MERS-CoV receptor DPP4 as a candidate binding target of the SARS-CoV-2 spike. Iscience 2020;23:101160. https://doi.org/10.1016/j.isci.2020.101160.

46. Bezzerri V, Gentili V, Api M, et al. SARS-CoV-2 viral entry and replication is impaired in cystic fibrosis airways due to ACE2 downregulation. Nat Commun 2023;14:132. https://doi.org/10.1038/s41467-023-35862-0.

47. Gasparello J, Marzaro G, Papi C, et al. Effects of sulforaphane on SARS-CoV-2 infection and NF-κB dependent expression of genes involved in the COVID-19 'cytokine storm'. Int J Mol Med 2023;52:76. https://doi.org/10.3892/ijmm.2023.5279.

48. Yan Y, Tao H, He J, Huang SY. The HDOCK server for integrated protein-protein docking. Nat Protoc 2020;15:1829–52. https://doi.org/10.1038/s41596-020-0312-x.

49. Abraham MJ, Murtola T, Schulz R, et al. GROMACS: high performance molecular simulations through multi-level parallelism from laptops to supercomputers. SoftwareX 2015;1–2:19–25. https://doi.org/10.1016/j.softx.2015.06.001.

50. The PLUMED consortium. Promoting transparency and reproducibility in enhanced molecular simulations. Nat Methods 2019;16:670–3. https://doi.org/10.1038/s41592-019-0506-8.

51. Huang J, Rauscher S, Nawrocki G, et al. CHARMM36m: an improved force field for folded and intrinsically disordered proteins. Nat Methods 2017;14:71–3. https://doi.org/10.1038/nmeth.4067.

52. Marrink SJ, Risselada HJ, Yefimov S, Tieleman DP, de Vries AH. The MARTINI force field: coarse grained model for biomolecular simulations. J Phys Chem B 2007;111:7812–24. https://doi.org/10.1021/jp071097f.

53. de Jong DH, Liguori N, van den Berg T, Arnarez C, Periole X, Marrink SJ. Atomistic and coarse grain topologies for the cofactors associated with the photosystem II core complex. J Phys Chem B 2015;119:7791–803. https://doi.org/10.1021/acs.jpcb.5b00809.

54. Dutta S, Panthu B, Chandra A. All-atom simulations of human ACE2-spike protein RBD complexes for SARS-CoV-2 and some of its variants: nature of interactions and free energy diagrams for dissociation of the protein complex. J Phys Chem B 2022;126:5375–89. https://doi.org/10.1021/acs.jpcb.2c00833.

55. Sun SC, Ley SC. New insights into NF-κB regulation and function. Trends Immunol 2008;29:469–78. https://doi.org/10.1016/j.it.2008.07.003.

56. Lawrence T. The nuclear factor NF-κB pathway in inflammation. Cold Spring Harb Perspect Biol 2009;1:a001651. https://doi.org/10.1101/cshperspect.a001651.

57. Liu T, Zhang L, Joo D, Sun SC. NF-κB signaling in inflammation. Signal Transduct Target Ther 2017;2:17023. https://doi.org/10.1038/sigtrans.2017.23.

58. Scheller J, Chalaris A, Schmidt-Arras D, Rose-John S. The pro- and anti-inflammatory properties of the cytokine interleukin-6. Biochim Biophys Acta 2011;1813:878–88. https://doi.org/10.1016/j.bbamcr.2011.01.034.

59. Pelaia C, Tinello C, Vatrella A, De Sarro G, Pelaia G. Lung under attack by COVID-19-induced cytokine storm: pathogenic mechanisms and therapeutic implications. Ther Adv Respir Dis 2020;14:1753466620933508. https://doi.org/10.1177/1753466620933508.

60. Walter PB, Fung EB, Killilea DW, et al. Oxidative stress and inflammation in iron-overloaded patients with beta-thalassaemia or sickle cell disease. Br J Haematol 2006;135:254–63. https://doi.org/10.1111/j.1365-2141.2006.06277.x.

61. Vinchi F, Sparla R, Passos ST, et al. Vasculo-toxic and pro-inflammatory action of unbound haemoglobin, haem and iron in transfusion-dependent patients with haemolytic anaemias. Br J Haematol 2021;193:637–58. https://doi.org/10.1111/bjh.17361.

62. Khan S, Shafiei MS, Longoria C, Schoggins JW, Savani RC, Zaki H. SARS-CoV-2 spike protein induces inflammation via TLR2-dependent activation of the NF-κB pathway. Elife 2021;10:e68563. https://doi.org/10.7554/eLife.68563.

63. Liu JJ, Hou SC, Shen CK. Erythroid gene suppression by NF-κB. J Biol Chem 2003;278:19534–40. https://doi.org/10.1074/jbc.M212278200.

64. Lee WH, Chung MH, Tsai YH, Chang JL, Huang HM. Interferon-γ suppresses activin A/NF-E2 induction of erythroid gene expression through the NF-κB/c-Jun pathway. Am J Physiol Cell Physiol 2014;306:C407–14. https://doi.org/10.1152/ajpcell.00312.2013.

65. Marzaro G, Lampronti I, D'Aversa E, et al. Design, synthesis and biological evaluation of novel trimethylangelicin analogues targeting nuclear factor kB (NF-κB). Eur J Med Chem 2018;151:285–93. https://doi.org/10.1016/j.ejmech.2018.03.080.

66. Lampronti I, Bianchi N, Zuccato C, et al. Increase in gamma-globin mRNA content in human erythroid cells treated with angelicin analogs. Int J Hematol 2009;90:318–27. https://doi.org/10.1007/s12185-009-0422-2.

67. Lechuga GC, Souza-Silva F, Sacramento CQ, et al. SARS-CoV-2 proteins bind to hemoglobin and its metabolites. Int J Mol Sci 2021;22:9035. https://doi.org/10.3390/ijms22169035.

68. Hatamleh MI, Chenna VSH, Contractor H, et al. Efficacy of hydroxyurea in transfusion-dependent major β-thalassemia patients: a meta-analysis. Cureus 2023;15:e38135. https://doi.org/10.7759/cureus.38135.

69. Malik JA, Ahmed S, Mir A, et al. The SARS-CoV-2 mutations versus vaccine effectiveness: new opportunities to new challenges. J Infect Public Health 2022;15:228–40. https://doi.org/10.1016/j.jiph.2021.12.014.

70. Zhang J, Cai Y, Xiao T, et al. Structural impact on SARS-CoV-2 spike protein by D614G substitution. Science 2021;372:525–30. https://doi.org/10.1126/science.abf2303.

71. Istifli ES, Netz PA, Tepe AS, Sarikurkcu C, Tepe B. Understanding the molecular interaction of SARS-CoV-2 spike mutants with ACE2 (angiotensin converting enzyme 2). J Biomol Struct Dyn 2022;40:12760–12771doi. https://doi.org/10.1080/07391102.2021.1975569.

72. Khan MI, Baig MH, Mondal T, et al. Impact of the double mutants on spike protein of SARS-CoV-2 B.1.617 lineage on the human ACE2 receptor binding: a structural insight. Viruses 2021;13:2295. https://doi.org/10.3390/v13112295.

73. Khoshnood S, Ghanavati R, Shirani M, et al. Viral vector and nucleic acid vaccines against COVID-19: a narrative reviewFront. Microbiol 2022;13:984536. https://doi.org/10.3389/fmicb.2022.984536.

74. Chen K, Liu J, Heck S, Chasis JA, An X, Mohandas N. Resolving the distinct stages in erythroid differentiation based on dynamic changes in membrane protein expression during erythropoiesis. Proc Natl Acad Sci U S A 2009;106:17413–8. https://doi.org/10.1073/pnas.0909296106.
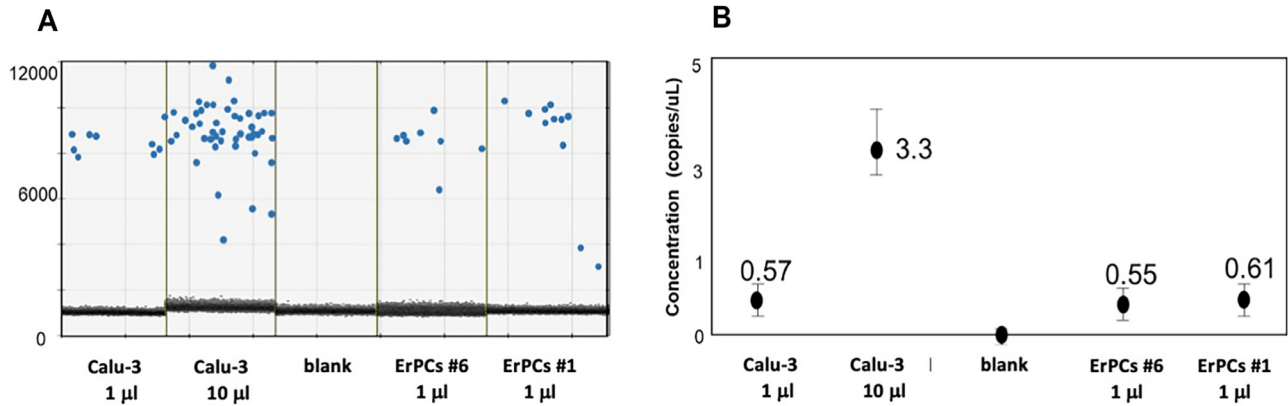
Figure S1 ACE2 expression in erythroid precursor cells (CD34+ ErPCs). ACE2 expression was assessed by RT-ddPCR using mRNAs extracted from CD34+ ErPCs isolated from β-thalassemia patients and compared with mRNA levels detected in Calu3 cells (used as ACE-2 expressing positive controls). Successful amplification of ACE2 is reported for each sample as blue spots (A); the concentration expressed in copies/μL is reported in (B).
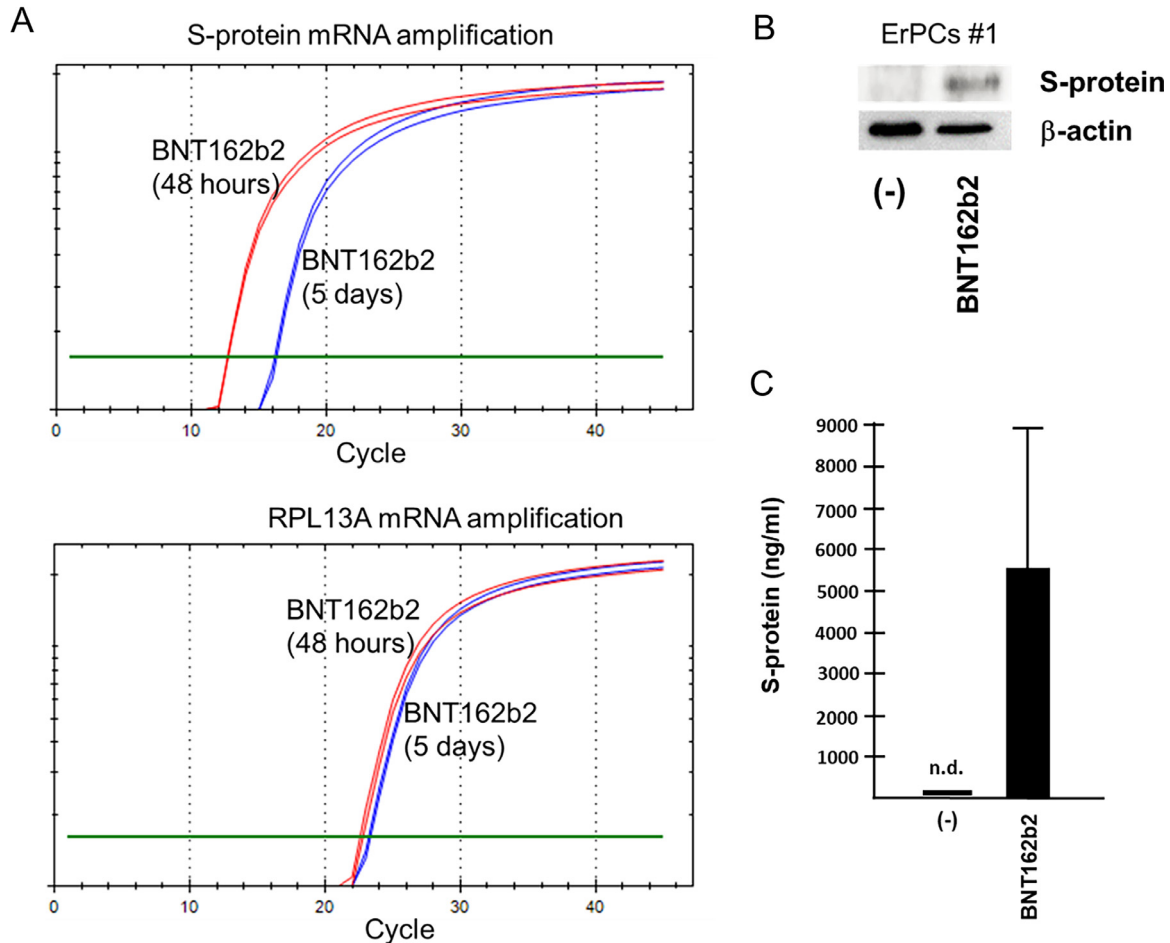
Figure S2 Spike expression in BNT162b2 treated ErPCs. (A) Representative data of Spike mRNA, upper part of the panel, and RPL13A mRNA (internal house-keeping control) analyzed by RT-qPCR in ErPCs #6 treated with COVID-19 BNT162b2 vaccine. The analyzed mRNAs were isolated after 48h (red curve) and 5 days (blue curve). (B) Representative example of evaluation of SARS-CoV-2 S-protein by Western blotting analysis. Protein analysis was performed on untreated and BNT162b2 vaccine-treated ErPCs #1 samples. Production of S-protein can be normalized after comparison with the amount of β-actin housekeeping protein. (C) The presence of SARS-CoV-2 Spike protein was assessed in the supernatant of untreated and BNT162b2 treated ErPCs (n=3) and analyzed by ELISA. In control untreated ErPCs S-protein was not detectable in all the experiments performed.
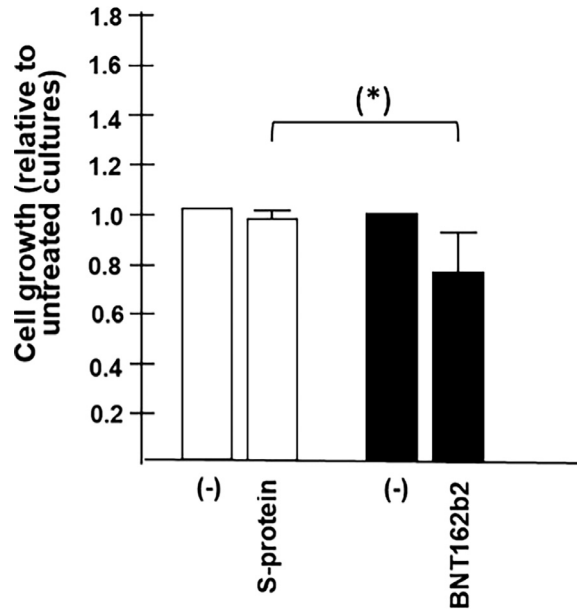
Figure S3 Effects on cell growth of the treatment of ErPCs with S-protein and BNT162b2. Data represent the mean ± S.D. values of cell number/ml, relative to control untreated (-) cells (n=5 and n=3 for S-protein and BNT162b2 treated ErPCs, respectively).
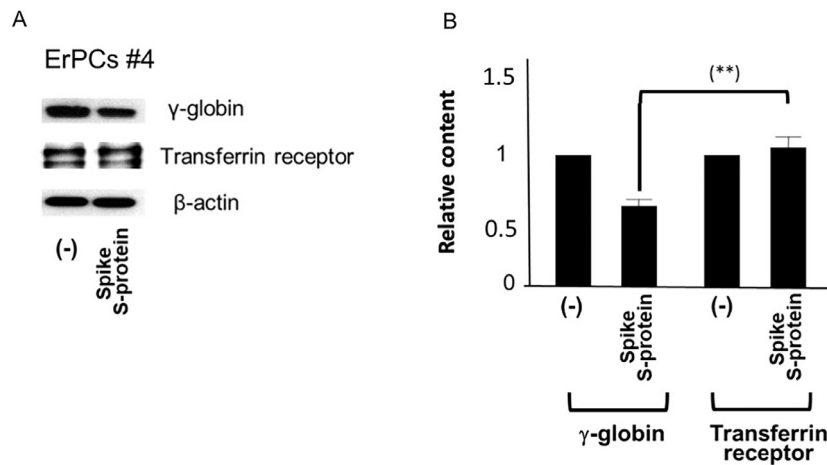
Figure S4 Treatment of ErPCs with SARS-CoV-2 S-protein: effect on Transferrin receptor (TrfR). (A) Representative Western blotting analysis of γ-globin and transferrin receptor CD 71 (TrfR and soluble TrfR) performed on lysates of ErPCs #4, either untretad (-) or treated with 20 nM S-protein. (B) Quantitative densitometric analyses of three independent experiments performed using ErPCs from β-thalassemia patients #1, #2 and #4. Results represent the mean ± S.D. of γ-globin/β-actin and TrfR/β-actin values relative to untreated (-) controls.